Available online at www.sciencedirect.com
SCIENCE DIRECT®
Journal of Organometallic Chemistry 690 (2005) 5881–5891
Journal of Organometallic Chemistry
www.elsevier.com/locate/jorganchem

Zinc *N*-heterocyclic carbene complexes and their polymerization of D,L-lactide

Tryg R. Jensen [a], Chris P. Schaller [b], Marc A. Hillmyer [a,*], William B. Tolman [a,*]

[a] *Department of Chemistry, University of Minnesota, 207 Pleasant Street SE, Minneapolis, MN 55455, USA*
[b] *Department of Chemistry, College of St. Benedict/St. John's University, 37S College Avenue, St. Joseph, MN 56374, USA*

Received 21 June 2005; received in revised form 20 July 2005; accepted 20 July 2005
Available online 16 September 2005

Abstract

A series of zinc complexes of monodentate *N*-heterocyclic carbenes (NHCs) and a new sterically bulky bidentate pyridyl-NHC ligand have been synthesized and characterized by spectroscopic and X-ray crystallographic methods. Dinuclear alkoxide complexes of monodentate NHC complexes with 2,4,6-trimethylphenyl substituents appear to form monomeric species in solution and show good control and activity for lactide polymerization, including mild stereoelectivity as indicated by formation of heterotactic-enriched polylactide in D,L-lactide polymerizations. Kinetics studies revealed an overall second order rate law, first order in [LA] and [catalyst]. Efforts to obtain Zn–alkoxide complexes of a more sterically hindered NHC with 2,6-diisopropylphenyl groups were unsuccessful due to Zn–NHC bond scission. Ligand dissociation was also observed in attempts to prepare Zn–alkoxide complexes of the bidentate pyridyl-NHC system, despite its chelating nature.

Keywords: Zinc; *N*-heterocyclic carbenes; Polymerization catalysis; Lactide, Polylactide

1. Introduction

N-heterocylic carbenes (NHC's) are now ubiquitous in their use as ligands for transition metals [1]. Although they are strong sigma donors analogous to phosphine ligands, NHC's are generally less labile. Pd- and Ru–N-heterocylic carbene complexes have been used for C–C coupling reactions and reactions involving olefin metathesis; systems employing NHC ligands have shown superior performance in many cases, and chiral NHC's have demonstrated promise in asymmetric catalysis [2,3].

Polylactide (PLA) is a biodegradable polymer produced by the ring-opening polymerization of lactide (LA). Because LA can be obtained through fermentation of corn and soybeans, production of PLA does not depend on the consumption of petrochemical feedstocks but is instead based on renewable resources [4]. PLA is currently produced commercially for food packaging; a number of biomedical applications have also been developed. Ideally, an LA polymerization catalyst should not only induce rapid polymerization of LA, but should also demonstrate control of PLA molecular weight and stereochemistry. A number of recent efforts have focused on the development of single site metal alkoxides for this purpose [5]. Aluminum alkoxides with supporting salen-type ligands have shown good control of tacticity in the production of PLA from racemic D,L-LA and from *meso*-LA but require high temperatures and long reaction times for adequate conversion [6]. On the other hand, zinc complexes are more active but demonstrate less control over tacticity [7,8]. Consequently, additional

* Corresponding authors. Tel.: +1 612 625 7834/4061; fax: +1 612 624 7029.
E-mail addresses: hillmyer@chem.umn.edu (M.A. Hillmyer), tolman@chem.umn.edu (W.B. Tolman).

0022-328X/$ - see front matter © 2005 Elsevier B.V. All rights reserved.
doi:10.1016/j.jorganchem.2005.07.070

investigation is warranted to determine factors conducive to rapid and well-controlled polymerization of LA.

As part of an ongoing effort to address these issues [9], we are exploring the use of Zn complexes of NHC's as LA polymerization catalysts. The synthesis of NHC complexes of diethyl zinc and bis(pentamethylcyclopentadienyl) zinc have been reported previously [10]. A recent report detailed several zinc complexes of 1,3-bis(2,4,6-trimethylphenyl)imidazol-2-ylidene and their homopolymerizations of ε-caprolactone and cyclohexene oxide, and copolymerizations of cyclohexene oxide and carbon dioxide [11]. Work on the coupling of epoxides and carbon dioxide with ill-defined imidazolium halide/zinc halide complexes has also been reported [12].

In our continuing studies of *N*-heterocyclic carbene zinc complexes and LA polymerization [13] we have pursued a number of different avenues designed to address issues of catalyst stability and selectivity. We report herein the development of synthetic routes to a series of such complexes and studies of their LA polymerization behavior. Because the relative lability of zinc complexes raised the possibility that the NHC ligand could dissociate from these initiators, we also employed a new bidentate pyridyl-NHC ligand.

2. Results and discussion

2.1. Complexes of monodentate NHC ligands

We recently reported the synthesis of a new NHC complex of zinc, **4a**, which was highly active in the polymerization of lactide. The alkoxide complex **4a** was prepared through alcoholysis of the previously reported [10a] NHC zinc diethyl complex **3a** (Scheme 1). Compound **3a**, in turn, was made by deprotonation of the 1,3-dimesitylimidazolium salt **1a** to provide the stable, isolable carbene **2a**, which was then coordinated to diethylzinc. Complex **4a** was fully characterized, including by X-ray crystallography; the structure is reproduced for comparative purposes (vide infra) in Fig. 1(a). ^{1}H NMR spectroscopy in THF-d_8 revealed two mesityl CH_3 resonances and one resonance due to the methylene group of the alkoxide ligand, consistent with either a monomeric structure or a highly fluxional dimer in solution.

We have now turned to another, somewhat simplified synthetic approach that has led to several new complexes **5a**,**b** and **6a** (Scheme 1). Rather than deprotonating the starting imidazolium salt and isolating the resulting carbene before metal complexation, diethylzinc was reacted directly with the appropriate imidazolium salts. This protocol has been demonstrated previously with the non-bulky 1,3-bis(methyl)imidazolium bromide and diethyl zinc [14]. In this way, the monomeric (NHC)Zn(Cl)Et complex **5a** was prepared from 1,3-mesitylimidazolium chloride and diethylzinc in high yield (91%). Spectroscopically pure **5a** was then treated with one equivalent of benzyl alcohol to afford dinuclear **6a** (77%).

A single crystal X-ray structure determination of **6a** (Fig. 1(b)) showed a number of similarities with **4a**. Both complexes are dimeric in the solid state and in both cases the two zinc atoms are bridged by alkoxide oxygen atoms. Both cores share C_2 symmetry about the bridging O–O interatomic axis, and in both cases this symmetry is broken by the capping NHC ligands, which are almost perpendicular to each other in the case of **6a**. The zinc–carbon bond distances, 2.040 Å in **6a** and 2.054 Å in **4a**, are typical; distances of 2.022–2.096 Å have been reported elsewhere [10,11]. However, the zinc–zinc distance is noticeably shorter in **6a** (2.935 Å) than in **4a** (3.021 Å), indicative of a more tightly coupled dimeric structure for the former complex.

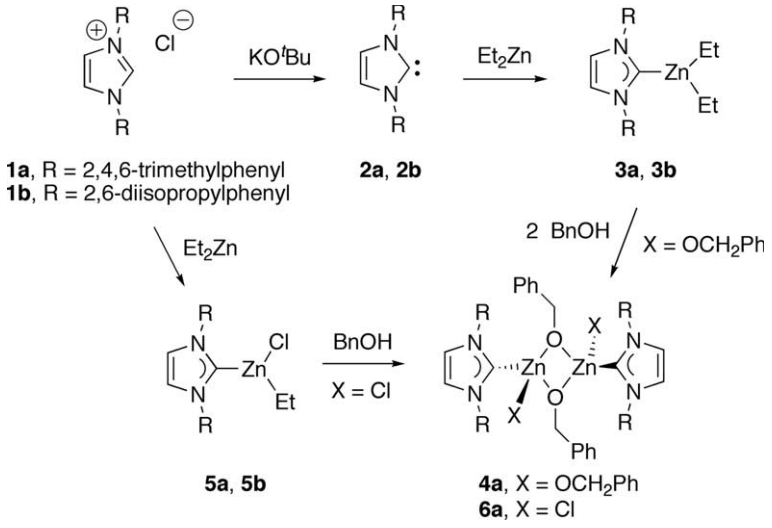

Scheme 1.

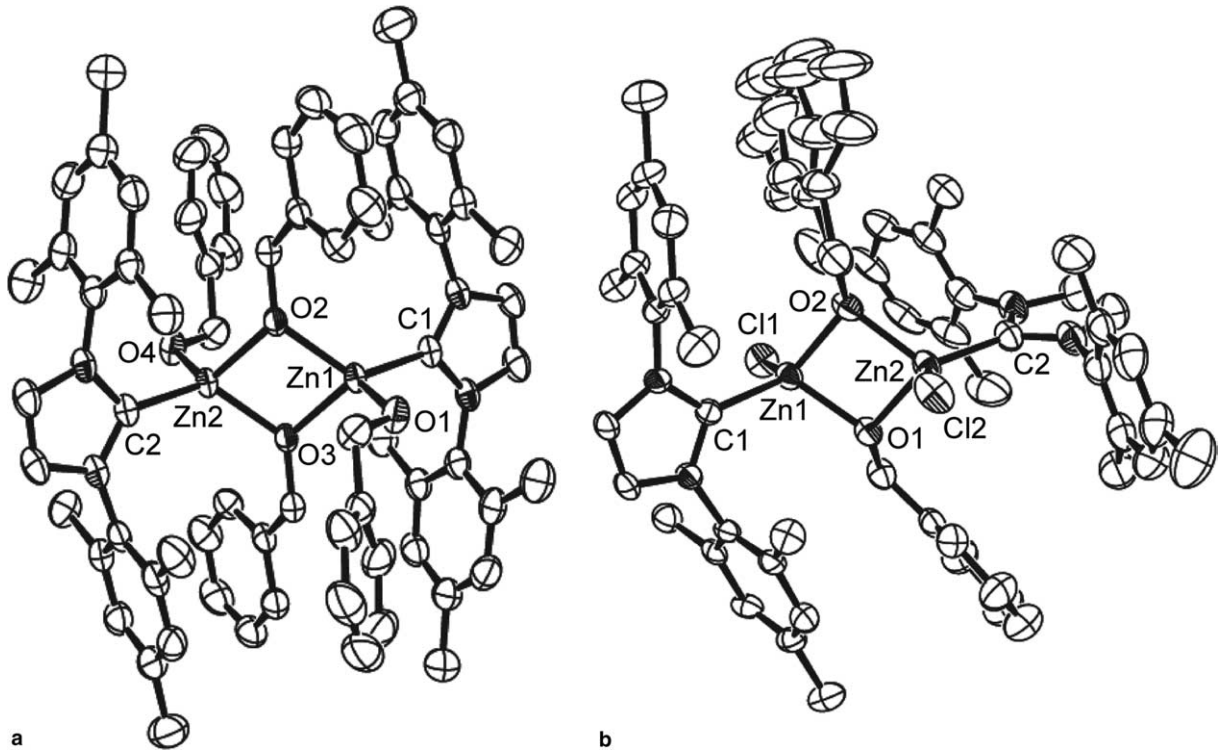

Fig. 1. Representations of the X-ray crystal structures of (a) **4a** (from [13]) and (b) **6a**, showing non-hydrogen atoms as 50% thermal ellipsoids. Selected bond distances (Å) and angles (deg): **4a**: Zn1–O1, 2.0135(14); Zn1–O2, 1.9198(15); Zn1–C1, 2.054(2); Zn1–Zn2, 3.0211(6); O1–Zn1–O2, 112.31(7); O2–Zn1–O3, 81.98(6); Zn1–O2–Zn2, 98.02(6); O2–Z1–C1, 124.80(8); O1–Zn1–C1, 107.75(7). **6a**: Zn1–Cl1 = 2.2619(10); Zn1–O1 = 1.983(2); Zn1–C1 = 2.040(3); Zn1–Zn2 = 2.9351(6); O1–Zn1–O2 = 84.65(10); Cl1–Zn1–O1 = 108.60(7); Zn1–O1–Zn2 = 96.12(10); O1–Z1–C1 = 115.80(11); Cl1–Zn1–C1, 108.97(10).

In addition, the solution structure of **6a** as determined by ^{1}H NMR spectroscopy in THF-d_8 is more complicated than that of **4a** and exhibits a concentration dependence. At high concentration ([**6a**] = 20 mM), the principal species (80%) displays two doublets in the PhC**H**$_2$O region of the spectrum, indicating inequivalent benzylic protons, but only two mesityl CH_3 resonances are observed [15]. At lower concentrations, a minor species becomes increasingly prevalent (50% at [**6a**] = 2 mM). This species displays equivalent benzylic protons but also two inequivalent resonances for the Ar–H and mesityl *ortho*-CH_3 positions. The ratio of these two species can be altered reversibly either by diluting with THF-d_8 or by adding more **6a**. We speculate that the species predominating at high concentration is the dimer with bridging benzyloxide ligands observed in the solid state, with the species growing in at lower concentration being a monomer, presumably (NHC)Zn(Cl)OBn. Interestingly, however, coalescence of the signals for these two species was not observed in THF solutions at temperatures as high as 55 °C, suggesting a relatively high energy barrier for their interconversion.

An investigation of the polymerization of D,L-LA initiated by complexes **4a** and **6a** in CH_2Cl_2 at 25 °C revealed good control over polymer molecular weight, which grew linearly with increasing LA conversion (Fig. 2). Molecular weights relative to polystyrene were generally consistent with one growing chain per alkoxide ligand (four growing chains per dimeric zinc complex **4a** and two growing chains per dimeric complex **6a**). The reaction resulted in a narrow molecular weight distribution, with a polydispersity index (PDI) resulting from initiation by **4a** of approximately 1.2 at lactide conversions up to 96%. The polydispersity index was slightly

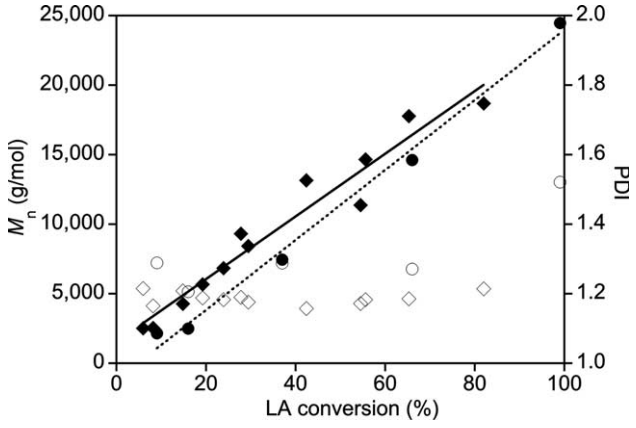

Fig. 2. Molecular weight (M_n, filled markers) and polydispersity index (PDI, open markers) of PLA produced using **4a** (diamonds) and **6a** (circles) as initiators. Linear fits of molecular weight vs. LA conversion are shown as solid (**4a**) or dashed (**6a**) lines.

higher when **6a** was used as an initiator and this value increased substantially later in the reaction.

Table 1 illustrates the results of further analysis of PLA produced using **4a** and **6a** as initiators. Complex **6a** was much more soluble in THF and CH_2Cl_2 than **4a**, allowing more straightforward comparisons of polymerizations for **6a** performed with different monomer:initiator ratios at a constant starting concentration of LA. At all catalyst loadings, the molecular weight of polymer produced was in good agreement with weights calculated based on one growing chain per initiating alkoxide ligand. Analysis of a sample at 10% conversion showed very good agreement between the theoretical molecular weight (1980 g/mol) and the experimental molecular weight obtained both by size exclusion chromatography (2.0 kg/mol) and by mass spectrometry (base peak at 2149 g/mol, corresponding to $HO(CHMeCO)_{14}OCH_2Ph \cdot Na^+$, as well as peaks corresponding to other oligomers). The latter result confirmed the presence of a benzyloxide initiating group in the polymer chain and also revealed a small fraction of chains containing odd numbers of lactic acid units, which indicates some degree of transesterification processes. Polydispersity indices were moderately narrow, and were especially low at high catalyst loading (PDI = 1.18 when $[LA]_0/[Zn]_0 = 50$). However, the polydispersity index increased greatly at longer reaction times.

Further mechanistic insight was obtained by kinetic analysis of the polymerizations initiated by **4a** and **6a**. We previously reported that the reaction with **4a** was very fast, with $k_{obs} = 1.9 \times 10^{-3}$ s^{-1} at $[LA]_0 = 1$ M and $[\mathbf{4a}]_0 = 2.7$ mM ($[Zn]_0 = 5.3$ mM). The reaction with **6a** occurs at essentially the same rate at a very similar concentration ($k_{obs} = 2.0 \times 10^{-3}$ s^{-1} at $[\mathbf{6a}]_0 = 2.5$ mM). These rates approach that of the fastest reported Zn catalyst [9a], which is about five times more rapid at the same monomer and catalyst loading ($k_{obs} = 1.2 \times 10^{-2}$ s^{-1} with $[LA]_0 = 1$ M and $[Zn]_0 = 5.3$ mM). During polymerization with either **4a** or **6a**, consumption of LA may be fit to an expression for first-order decay, but with **6a** a small but reproducible inflection point is observed in the initial part of the curve in a plot of [LA] vs. time, indicating autocatalysis or an induction period (Fig. 3). Given the complicated structure of **6a** indicated by its NMR spectra (vide supra), it is possible that a zinc dimer/monomer equilibrium is responsible for this behavior.

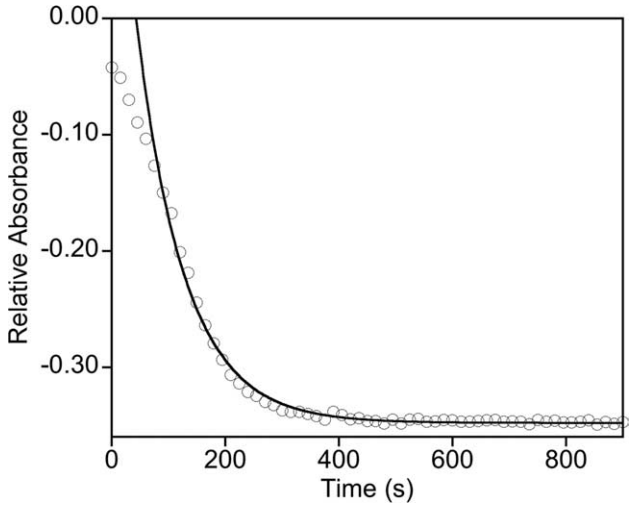

Fig. 3. Consumption of LA over time during polymerization by **6a** at 25 °C in THF, monitoring LA at 1775 cm^{-1} by FT-IR spectroscopy ($[LA]_0 = 1$ M, $[Zn]_0 = 15$ mM). The line is a non-linear fit of the data (except the first 5 points) to the first order expression $A_t = (A_0 - A_\infty)e^{-kt} + A_\infty$, which yielded $k_{obs} = 0.0119$ s^{-1} ($R^2 = 0.993$).

In further kinetic studies, k_{obs} values for the polymerization of LA by **6a** were obtained at various initial catalyst concentrations. A linear fit of the data (Fig. 4) is consistent with a rate law that is first order in $[Zn]_0$ and second order overall, such that rate $= k_p[Zn][LA]$ and $k_p = 0.9$ M^{-1} s^{-1}, with a non-zero x intercept suggestive of a small amount of a catalyst deactivator (~3.7 mM) [9a,9d]. Indeed, polymerizations performed using concentrations of **6a** lower than those shown in Fig. 4 failed to go to full conversion ($[Zn]_0 = 2$ mM, $[LA_0]/[Zn]_0 = 500$). In these cases, initial consumption of LA was observed but the reaction ceased abruptly

Table 1
Data for the polymerization of D,L-LA by compounds **4a** and **6a**[a]

Catalyst	$[LA]_0/[Zn]_0$	Polymerization time (min)	LA conv. (%)[b]	Calculated M_n (kg/mol)	M_n (kg/mol)[c]	PDI (M_w/M_n)[c]	P_r[d]
4a	260	20	96	18.6	17	1.25	0.6
6a	200	16	97	28.0	30	1.38	0.6
6a	130	75	99	18.6	19	1.68	0.6
6a	130	4	99	18.6	20	1.52	0.6
6a	130	0.5	10	2.0	2.0; 2.2[e]	1.39	0.6
6a	50	2	95	7.0	7.4	1.18	0.6

[a] Conditions: CH_2Cl_2 at 25 °C; $[LA]_0 = 1$ M.
[b] Determined by ^{1}H NMR spectroscopy.
[c] SEC (relative to polystyrene in THF).
[d] Probability of racemic linkage between monomer units as determined from the methine region of the homonuclear decoupled ^{1}H NMR spectrum.
[e] Base peak in MALDI-TOF mass spectrum.

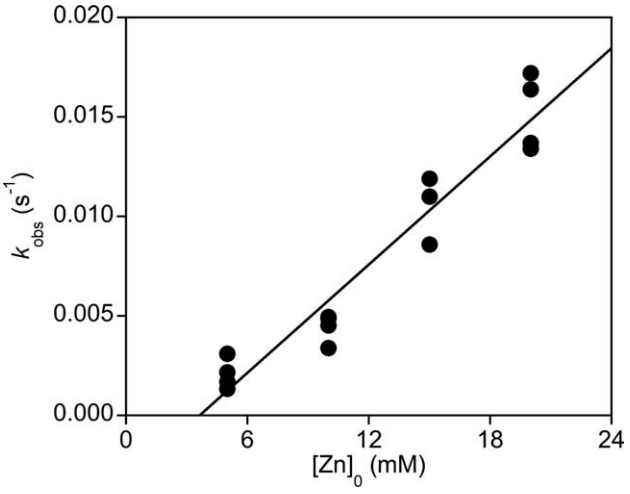

Fig. 4. Plot of pseudo-first order rate constants k_{obs} as a function of $[Zn]_0$ polymerizations of D,L-LA by **6a** at 25 °C in THF ($[LA]_0 = 1$ M). From the slope of the linear fit shown $k_p = 0.9\ M^{-1}$ ($R^2 = 0.93$).

after approximately 1 min. These data are consistent with catalyst deactivation at low catalyst loadings, similar to what had been seen previously for other systems [9a,9d], but in this case with the rate of deactivation being similar to the rate of LA polymerization.

^{1}H NMR analysis [16] showed that both **4a** and **6a** exhibit modest stereocontrol in the polymerization of D,L-LA, with a slight preference for racemic linkages between monomer units in the PLA chains ($P_r = 0.6$, Table 1). This stereobias presumably arises from chain-end control, since **4a** and **6a** contain no chiral centers. Thus, the orientation of an approaching LA unit is influenced by the stereochemistry of the last unit of LA previously incorporated. We speculated that this subtle stereochemical influence might be enhanced by increasing the steric bulk at the site of polymerization. Increased crowding at the site would exacerbate any interactions that favor one orientation of LA over another.

Consequently, we applied the synthetic strategies outlined above to prepare more sterically hindered zinc complexes of 1,3-bis(2,6-diisopropylphenyl)imidazol-2-ylidene (**2b**, Scheme 1). We previously reported the preparation of the zinc diethyl complex **3b**, prepared via a route analogous to **3a** [13]. The X-ray crystal structure of **3b**, unavailable at that time, is shown in Fig. 5(a). Alternatively, complex **5b** was prepared through direct addition of diethylzinc to the imidazolium chloride **1b**. This reaction proceeded in good yield to give a spectroscopically pure complex that was also characterized by X-ray crystallography (Fig. 5(b)). Both structures feature a monomeric species with a Zn(II) ion in a trigonal planar coordination environment. The Zn–C1 bond in **3b**, at 2.100 Å, is at the higher end of the range observed in other zinc carbene complexes (2.022–2.096 Å) [10,11]. This bond is presumably lengthened due to the steric influence of the neighboring isopropyl groups. The analogous bond in **5b** is somewhat shorter, however, at 2.032 Å. It may be that the two ethyl groups in **3b** exert a more dramatic steric effect than the single ethyl ligand and the chloride in **5b**, allowing the bulky NHC ligand to bind more tightly to **5b** see Fig. 6.

Unfortunately, treatment of either **3b** or **5b** with benzyl alcohol failed to result in alcoholysis of the zinc ethyl groups. The reaction of benzyl alcohol with **3b** instead yielded the liberated NHC **2b**. It may be that the steric bulk of the carbene ligand results in a zinc–carbon bond that is too weak to survive reaction with the strongly coordinating alcohol; addition of alcohol consequently results in ligand dissociation. On the other hand, the reaction of benzyl alcohol with **5b** resulted in a complex mixture of products, and it is unclear what role carbene dissociation may have played in that case.

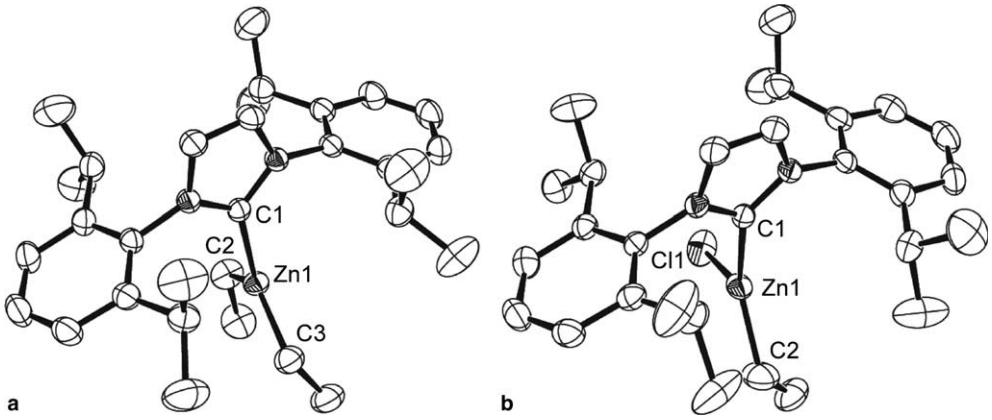

Fig. 5. Representations of the X-ray crystal structure of (a) **3b** and (b) **5b**, showing non-hydrogen atoms as 50% thermal ellipsoids. The hydrogen atoms are omitted for clarity. Selected bond distances (Å) and angles (°) for **3b**: Zn1–C1 = 2.1000(18); Zn1–C2 = 1.998(2); Zn1–C3 = 2.027(3); C1–Zn1–C2 = 117.62(9); C1–Zn1–C3 = 111.58(10); C2–Zn1–C3 = 129.83(12). Disorder in one of the ethyl groups that was modeled in the crystal structure solution is omitted here for clarity. **5b**: Zn1–C1 = 2.0319(16); Zn1–C2 = 1.979(2); Zn1–Cl1 = 2.2551(8); C1–Zn1–C2 = 132.99(9); C1–Zn1–Cl1 = 109.57(4); C2–Zn1–Cl1 = 117.42(8).

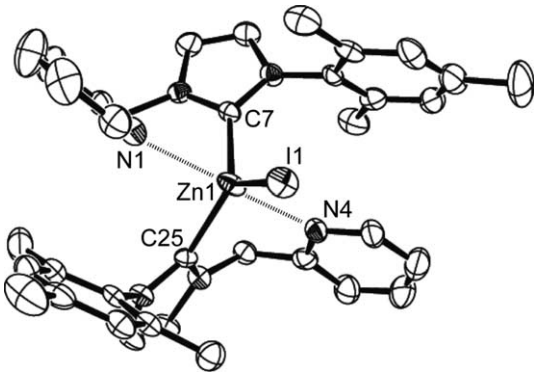

Fig. 6. Representation of the X-ray crystal structure of **9**, showing non-hydrogen atoms as 50% thermal ellipsoids. The hydrogen atoms and the anion are omitted for clarity. Selected bond distances (Å) and angles (°): Zn1–C7 = 2.049(6); Zn1–C25 = 2.055(6); Zn1–I1 = 2.5850(9); C7–Zn1–C25 = 113.7(2); C7–Zn1–N4 = 94.8(2); C25–Zn1–N4 = 83.7(2); C7–Zn1–I1 = 123.78(16); C25–Zn1–I1 = 122.35(16); N4–Zn1–I1 = 95.24(13). Selected interatomic distances (Å): Zn1–N1 = 2.557(6); Zn1–N4 = 2.408(5).

2.2. Complexes of a bidentate pyridyl-NHC ligand

In an effort to prevent the aforementioned ligand dissociation problem and further probe ligand structural effects on cyclic ester polymerization behavior, we turned our attention to multidentate NHC derivatives. A number of recent reports have underscored the utility of NHC ligands that incorporate chelating phenolic, alkoxide or pyridyl moieties [17]. In initial efforts toward this end, we synthesized a new, bidentate pyridyl-NHC ligand precursor **7** (Scheme 2). Thus, in a procedure similar to that reported previously for the preparation of 3-methyl-1-picolylimidazolium iodide [22], picolyl chloride was treated with sodium iodide and mesityl imidazole [23]. The resulting 3-mesityl-1-picolylimidazolium iodide, **7**, was formed in 84% yield and could be recrystallized in THF.

Isolating the imidazol-2-ylidene from structures similar to **7** has generally proven difficult because of multiple acidic protons in the molecule (e.g., the benzylic protons on the picolyl group) as well as radical rearrangements at the benzylic position [18]. Indeed, we were unable to isolate 3-mesityl-1-picolylimidazol-2-ylidene by addition of base to **7**. On the other hand, the reaction of **7** with diethylzinc resulted in the formation of either **8** or the bis-ligand adduct **9**, depending on the stoichiometry of the reaction and the temperature. Because of the volatility of diethylzinc and the heat required to induce ethane elimination, **9** was more commonly produced by the reaction of **8** with imidazolium salt **7**. Both the imidazolium salt **7** [15] and complex **9** were characterized by X-ray crystallography, and the structure of **9** is illustrated in Fig. 6 [19]. The Zn(II) ion is bound by two NHC-pyridyl ligands (albeit with long Zn–N(pyridyl) distances indicative of a weak bonding interaction) and one iodide bound to the zinc; the second iodide is present as a counter anion. The zinc–carbon bond lengths are both typical (2.049(6) and 2.055(6) Å) of reported values [10,13].

Unfortunately, reaction of the picolylcarbene zinc ethyl complex **8** with benzyl alcohol did not yield an alkoxide complex. At the same time, straightforward dissociation of the carbene ligand, as observed with complexes **3b** and **5b** of the non-chelating NHC ligands, did not occur here. Instead, protonation of the carbene ligand resulted in formation of the picolylimidazole salt **7**. The exact mechanism of this transformation is unclear because formation of **7** was accompanied by the appearance of intractable side products.

Despite this drawback, we were interested in seeing whether the complexes of bidentate carbene ligands initiated polymerization in the absence of alkoxide ligands. Although polymerization of lactide did not occur in solution, melt polymerizations of D,L-LA at 140 °C

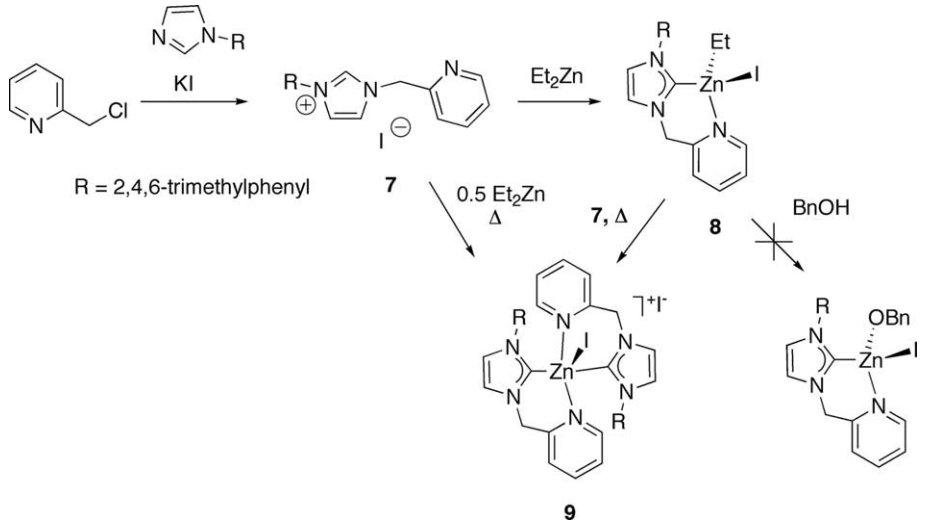

Scheme 2.

Table 2
Data for the polymerization of D,L-LA by compounds **7–9**[a]

Catalyst	$[LA]_0/[Zn]_0$	Polymerization time (min)	LA conv. (%)[b]	Calc. M_n (kg/mol)	M_n (kg/mol)[c]	PDI (M_w/M_n)[c]	P_r[d]
7	50	5	0				
7	200	5	0				
8	100	5	96	13.8	12	2.45	0.6
8	200	5	86	24.8	20	2.04	0.6
9	50	5	91	6.6	6.1	2.51	0.6
9	200	5	73	21.0	12	1.78	0.6

[a] Conditions: neat, 140 °C.
[b] Determined by ^{1}H NMR spectroscopy.
[c] SEC (relative to polystyrene in THF).
[d] Probability of racemic linkage between monomer units as determined from the methine region of the homonuclear decoupled ^{1}H NMR spectrum.

using **8** and **9** produced PLA (Table 2). The melt polymerization produces heterotatic enriched PLA ($P_r = 0.6$) with good conversion of LA at a rapid rate. The polydispersity indices are somewhat broad ($M_w/M_n = 1.75–2.45$), but the molecular weight distributions are monomodal. While alcohol impurities in the LA would probably cause **8** to degrade to the imidazolium salt, **7**, the latter does not initiate polymerization. It is still possible that some other type of decomposition of either **8** or **9** occurs to yield an active initiator, but at high catalyst loadings ($[LA]_0/[Zn]_0 \leqslant 100$) the similarity between calculated M_n and experimental M_n suggests that a single site catalyst is active.

The demonstrated lability of carbenes on zinc that we have described in this manuscript suggests it is reasonable to assume that some 1,3-bis(2,4,6-trimethylphenyl) imidazol-2-ylidene dissociation from complexes such as **6a** or **8** could occur. Given that 1,3-bis(2,4,6-trimethylphenyl)imidazol-2-ylidene in the presence of alcohol is known to be a rapid, stereoelective, and controlled polymerization catalyst of D,L-LA [13,20], there could be some concern that the polymerization we have observed is not due to zinc complexes, but to dissociated imidazol-2-ylidenes such as **2a**. However, as was shown previously with **4a**, the PLA formed from these reactions is heterotactic enriched ($P_r = 0.6$) while PLA made with 1,3-bis(2,4,6-trimethylphenyl)imidazol-2-ylidene is isotactic enriched [13]. This observation suggests that, while we cannot discount participation to some degree of 1,3-bis(2,4,6-trimethylphenyl)imidazol-2-ylidene, the main catalytic species in polymerizations catalyzed by **6a**, for example, must be distinctly different than the free carbene, 1,3-bis(2,4,6-trimethylphenyl)imidazol-2-ylidene.

3. Concluding remarks

The new NHC zinc alkoxide complex **6a** has been synthesized and characterized. It polymerizes D,L-LA with good control of molecular weight, high activity, and moderate stereoelectivity to make heterotactic-enriched PLA. The polymerization of D,L-LA by **6a** follows kinetics that are first order in [LA] and [**6a**].

Unlike some of the other late transition metals, zinc complexes of NHC's are prone to dissociation, particularly when the NHC is sterically bulky. For example, we found that addition of alcohol to **3b** and **5b** comprising the hindered 1,3-bis(2,6-diisopropylphenyl)imidazol-2-ylidene ligand failed to yield zinc alkoxides via alcoholysis of the zinc ethyl group. In at least one case, this complication resulted from dissociation of the carbene ligand. In order to counter problems with NHC ligand dissociation, a new imidazolium salt containing a pyridyl arm, **7**, was explored. Ligand **7** reacts directly with diethyl zinc to produce either the bidentate carbene complex **8** (at room temperature) or **9** (at elevated temperatures). While the use of chelation in **8** failed to prevent loss of the carbene ligand during alcoholysis, both **8** and **9** can polymerize D,L-LA in the melt with high activity to make heterotactic enriched PLA.

Continuing studies with NHC complexes of zinc should allow us to produce new catalysts capable of rapid, controlled, highly stereoelective LA polymerization, and provide further insight into the mechanism of metal-mediated LA polymerization. In particular, we will continue to examine other chelating NHC ligands on zinc in an effort to obtain complexes with greater stability towards decomposition during polymerization of lactide.

4. Experimental procedures

4.1. General procedures

All reactions were performed under a nitrogen atmosphere, using either standard Schlenk techniques or a dinitrogen-filled MBraun glovebox. All solvents and reagents were obtained from commercial sources and used as received unless otherwise stated. Pentane, dichloromethane, tetrahydrofuran and toluene were passed through purification columns (Glass Contour, Laguna, CA). Deuterated solvents (all 99 atom%D) were purchased from Cambridge Isotope Laboratories, dried over calcium hydride, distilled under vacuum, and stored under nitrogen. Benzyl alcohol was distilled from calcium hydride.

Diethyl zinc (1 M in hexanes) was purchased from Aldrich and used as received. D,L-Lactide was purified by recrystallization from toluene, followed by repeated (2–3×) vacuum sublimation. 1,3-bis(2,4,6-trimethylphenyl) limidazol-2-ylidene (**2a**), 1,3-bis(2,4,6-trimethylphenyl) limidazolium chloride (**1a**), 1,3-bis(2,6-diisopropylphenyl)imidazolium chloride (**1b**), and 1,3-bis(2,6-diisopropylphenyl)imidazol-2-ylidene were prepared as previously described [21]. The complexes **3a** [10a], **4a** [13], and **4b** [13] were prepared by established procedures.

NMR spectra were collected with a Varian VI-300, Varian VXR-300, or Varian VXR-500 spectrometer. Chemical shifts for ^{1}H and ^{13}C spectra were referenced using internal solvent resonances and are reported relative to tetramethylsilane. Elemental analyses were determined by Robertson Microlit Laboratories Inc., Madison, NJ. IR spectra for characterization were recorded on a Thermo Nicolet Avatar 370 FT-IR spectrometer, by ATR with a Ge crystal. Molecular weights (M_n and M_w) and polydispersity indices (PDI = M_w/M_n) were determined by size exclusion chromatography. Size exclusion chromatography (SEC) was performed using a Hewlett–Packard 1100 series liquid chromatograph with THF as the mobile phase. The SEC instrument was equipped with three Jordi divinylbenzene columns (pore sizes 500, 10^3, and 10^4 Å; column temperature 40 °C), and output was detected with an HP1047A differential refractive index detector, an eluent flow rate of 1 mL/min, and a 50 μL injection loop. The instrument was calibrated using narrow polydispersity polystyrene standards (Polymer Laboratories) with molecular weights ranging from 5000 to 1×10^6 g/mol.

4.1.1. General solution polymerization procedure

Glassware used for polymerizations was oven or flame-dried. In the glovebox a vial was charged with D,L-LA (375 mg, 2.59 mmol) and solvent (2.6 mL) with rapid stirring. Once the LA had dissolved, a solution of the catalyst was injected to start the reaction. After an appropriate time, the reaction mixture was poured into pentane to precipitate the polymer. Excess pentane was removed be decantation and the polymer mixture was dried at 80 °C prior to characterization by SEC and ^{1}H NMR spectroscopy.

4.1.2. General melt polymerization procedure

In the glovebox, a vial was loaded with a Teflon stir bar, D,L-LA, and the appropriate amount of catalyst, and the solid components were mixed thoroughly. The vial was capped tightly, and removed from the glovebox. The vial was submerged in an oil bath set at 140 °C. After the appropriate reaction time, the vial was quickly removed from the oil bath and dropped in a vacuum dewar filled with liquid nitrogen. When the nitrogen stopped boiling, the vial was removed. The polymer was scraped out with a screw driver or the glass vial was broken prior to characterization by SEC and ^{1}H NMR spectroscopy.

4.1.3. Kinetics measurements

The polymerization of D,L-LA was monitored by IR spectroscopy using a Mettler Toledo ReactIR 4000 spectrometer. A reaction flask was charged with LA and solvent in the glovebox (the total volume varied, but the average total volume was approximately 3.5 mL). The ReactIR probe was then attached to the flask via a ground glass joint, and the apparatus was removed from the glovebox and attached to the IR spectrometer so that the reaction flask was immersed in a temperature controlled bath at 24 °C with rapid stirring. The solution temperature was allowed to equilibrate over 5 min, and catalyst (as a solution prepared in the glovebox) was injected through a septum via syringe. Peaks due to LA at 1776 and 1250 cm^{-1} and peaks due to PLA at 1750 and 1184 cm^{-1} were monitored; analysis of LA decay and PLA growth gave very similar results. The observed rate constants (k_{obs}) were extracted by fitting an exponential curve to the plot of absorbance versus time (for the peak at 1776 cm^{-1}) using $A_t = (A_0 - A_\infty)e^{-kt} + A_\infty$, allowing A_0, A_∞, and k to vary freely. The data were analyzed over at least three half-lives. All linear and non-linear curve fits were performed with KaleidaGraph.

4.2. Ethyl-zinc-chloride · 1,3-bis(2,4,6-trimethylphenyl) imidazol-2-ylidene adduct (*5a*)

In a 19 mL vial in the glove box, 1,3-bis(2,4,6-trimethylphenyl)imidazolium chloride (**1a**, 1.00 g, 2.93 mmol) was dissolved in THF (50 mL). Diethylzinc (1.0 M in hexanes) was added by syringe (3.1 mL, 3.1 mmol). The solution was stirred at room temperature overnight. Volatiles were removed in vacuo to yield a white powder (1.2 g, 2.7 mmol, 91% yield). ^{1}H NMR (300 MHz, THF-d_8) δ −0.061 (q, $J = 8.1$ Hz, 2H), 0.69 (t, $J = 8.1$ Hz, 3H), 2.15 (s, 6H), 2.33 (s, 3H), 7.00 (s, 4H), 7.34 (s, 2H). *Anal.* Calc. for $C_{23}H_{29}ClN_2Zn$: C, 63.60; H, 6.73; N, 6.45. Found: C, 60.06; H, 6.39; N, 6.27%.

4.3. Dimer of benzyloxy-zinc-chloride · 1,3-bis(2,4,6-trimethylphenyl)imidazol-2-ylidene adduct (*6a*)

To a solution of **5a** (750 mg, 1.72 mmol) in cold THF (3 mL, −35 °C) was slowly added a solution of benzyl alcohol (186 mg, 1.72 mmol, in 2 mL THF, −35 °C). The resulting pale, yellow solution was stirred for 3 h, the solvent volume was concentrated in vacuo to 2 mL, and the product was precipitated with cold pentane (15 mL) and collected by filtration to obtain an off-white product (680 mg, 1.33 mmol, 77%). Single crystals for examination by X-ray diffraction were grown by cooling a THF solution to −40 °C. ^{1}H NMR (300 MHz, THF-d_8): δ 7.0–7.25 (m, 5H), 7.09

(s, 2H), 6.49 (s, 4H), 3.49 (d, $J = 16$ Hz, 1H), 3.30 (d, $J = 16$ Hz, 1H), 2.10, (s, 6H), 1.85 (s, 12H) ppm. $^{13}C\{^1H\}$ NMR (300 MHz, THF-d_8): 177.1, 149.1, 139.1, 136.1, 129.9, 129.8, 127.4, 126.4, 124.7, 124.5, 35.1, 23.3, 21.4 ppm. IR: 3030(w), 2930(m), 1490(m), 1063(s),739(s) cm^{-1}. *Anal.* Calc. for $C_{56}H_{62}Cl_2N_4O_2Zn_2$: C, 65.63; H, 6.10; N, 5.47. Found: C, 63.06; H, 6.19; N, 5.24%.

4.4. Ethyl-zinc chloride · 1,3-bis(2,6-diisopropylphenyl) imidazol-2-ylidene adduct (**5b**)

In a 19 mL vial in the glove box 1,3-bis(2,6-diisopropylphenyl)imidazolium chloride (**1b**, 0.321 g, 0.733 mmol) was suspended in THF (10 mL) and cooled to −40 °C. Diethylzinc (1.0 M in hexanes) was added by syringe (1.1 mL, 1.1 mmol). The solution was allowed to warm to room temperature over 20 min. The reaction was stirred for another 60 min at room temperature. The solvent volume was reduced to ~2 mL, the product was precipitated by adding the mixture to Et_2O (15 mL), and then collected by filtration to obtain an off-white powder (0.34 g, 0.66 mmol, 90% yield). Single crystals were grown by slowing cooling a toluene solution. ^1H NMR (300 MHz, THF-d_8) δ −0.52 (q, $J = 8.1$ Hz, 2H), 0.68 (t, $J = 8.1$ Hz, 3H), 1.18 (d, $J = 6.9$ Hz, 12H), 1.28 (d, $J = 6.9$ Hz, 12H), 2.6 (sept, $J = 6.9$ Hz, 4H), 7.25 (s, 2H), 7.32 (s, 2H), 7.35 (s, 4H). *Anal.* Calc. for $C_{29}H_{41}ClN_2Zn$: C, 67.18; H, 7.97; N, 5.40. Found: C, 66.10; H, 7.93; N, 5.39%.

4.5. 1-Mesityl-3-picolylimidazolium iodide (7)

1-Mesityl-3-picolylimidazolium iodide was synthesized with minor modification to a similar procedure [22]. To a solution of picolyl chloride, prepared by treating picolyl chloride hydrochloride (4.63 g, 28.2 mmol) with sodium hydrogen carbonate (4.19 g, 49.9 mmol) in 200 mL of acetone were added 1-mesityl imidazole [23] (5.01 g, 25.1 mmol) and NaI (4.63 g, 30.9 mmol). After the mixture was stirred for 36 h, volatiles were removed in vacuo. The solid was dissolved in dichloromethane (100 mL), and the solution filtered through Celite. Addition of diethyl ether (400 mL) caused a solid to precipitate. The solvent was removed by filtration, the solid taken up in dichloromethane (100 mL), and diethyl ether (400 mL) added to precipitate the product. After filtration, drying in vacuo yielded a yellow/orange solid (9.63 g, 84%). Single crystals were grown by slow evaporation from a THF solution. ^1H NMR (500 MHz, $CDCl_3$, 21 °C): δ 9.82 (s, 1H), 8.50 (s, 1H), 8.13 (s, 1H), 7.80 (m, 1H), 7.74 (m, 1H), 7.31 (m, 2H), 7.00 (s, 2H), 6.09 (s, 2H), 2.34 (s, 3H), 2.09 (s, 6H). $^{13}C\{^1H\}$ NMR (75 MHz, $CDCl_3$): δ 152.2, 149.8, 141.4, 137.7, 137.6, 134.3, 130.6, 129.9, 124.3, 124.0, 123.8, 122.8, 54.0, 21.2, 17.8. *Anal.* Calc. for $C_{18}H_{20}IN_3$: C, 53.34; H, 4.97; N, 10.37. Found: C, 53.11; H, 4.76; N, 10.24%.

4.6. Ethyl-zinc iodide · 1-mesityl-3-picolyl imidazol-2-ylidene adduct (**8**)

In a 120 mL vial in the glove box, diethylzinc (1.0 M in hexanes) was added by syringe (5.9 mL, 5.9 mmol, 1.2 equiv.) to THF (100 mL) at −40 °C and stirred for 30 s. Compound **7** (2.00 g, 4.94 mmol) was added to the solution. The solution was stirred at room temperature overnight and everything dissolved. The solution was transferred to a 500 mL Erlenmeyer and pentane (300 mL) was added to precipitate a solid. The solid was filtered, washed consecutively with pentane (50 mL), toluene (20 mL), pentane (20 mL) and dried in vacuo to yield a white powder (2.11 g, 4.2 mmol, 86% yield). An analytically pure sample was made by reprecipitation in THF. ^1H NMR (300 MHz, THF-d_8) δ −0.153 (q, $J = 8.1$ Hz, 2H), 0.822 (t, $J = 8.1$ Hz, 3H), 1.98 (s, 6H), 2.31 (s, 3H), 5.93 (s, 2H), 6.97 (s, 2H), 7.12 (d, $J = 1.8$ Hz, 1H), 7.45 (m, 1H), 7.75–7.85 (m, 2H), 7.92 (m, 1H), 8.62 (m, 1H). $^{13}C\{^1H\}$ NMR (75 MHz, C_6D_6, 22 °C) δ 182.0, 155.6, 150.6, 140.1, 140.0, 136.1, 130.5, 129.9, 125.8, 125.5, 125.0, 123.7, 121.6, 52.5, 21.3, 18.3, 14.0, 0.4. *Anal.* Calc. for $C_{20}H_{24}IN_3Zn$: C, 48.17; H, 4.85; N, 8.43; I, 25.45; Zn, 13.11. Found: C, 48.01; H, 4.69; N, 8.29%.

4.7. $(C_{18}H_{19}N_3)_2ZnI^+$ I^- (**9**)

A 100 mL Schlenk flask in the glove box was charged with **8** (0.221 g, 0.44 mmol), **7** (0.173 g, 0.43 mmol), and toluene (50 mL). The flask was heated with stirring to 110 °C for 3 h; the solution becomes homogeneous. The reaction was allowed to cool to room temperature. The solid was filtered and wash consecutively with toluene (50 mL) and pentane (30 mL) before being dried in vacuo to yield a white powder (0.33 g, 0.36 mmol, 83% yield). Single crystals of **9** were grown by slow evaporation of a pentane solution into a THF solution of **9**. ^1H NMR (300 MHz, acetonitrile-d^8) δ 2.05 (s, 2H), 2.35 (s, 6H), 5.60 (s, 4H), 7.12 (s, 4H), 7.37 (m, 2H), 7.45 (d, $J = 2.1$ Hz, 2H), 7.52 (m, 2H), 7.70 (d, $J = 2.1$ Hz, 2H), 7.86 (m, 2H), 8.54 (m, 2H). *Anal.* Calc. for $C_{36}H_{38}IN_6Zn$: C, 49.48; H, 4.38; N, 9.62; I, 29.06; Zn, 7.48. Found: C, 49.83; H, 4.53; N, 9.39%.

Acknowledgements

Financial support from the NSF (CHE-023666) is gratefully acknowledged. C.P.S. wishes to acknowledge support from the NSF-RSEC program at the University of Minnesota. We thank Lyndal M.R. Hill, Benjamin E. Kucera, Victor G. Young, Jr., and the X-ray Crystallo-

graphic Laboratory at the University of Minnesota for the crystallographic determinations, and Dana Reed for assistance with mass spectrometry.

Appendix A. Supplementary data

NMR spectra for **6a** and a representation of the X-ray crystal structure of **7** are provided. Crystallographic data (CIFs) for the structural analyses have been deposited with the Cambridge Cystallographic Data Centre (CCDC No. 275448 for compound **3b**, No. 275331 for compound **5b**, No. 275452 for compound **7**, Nos. 275450 and 275449 for compound **9** (forms 1 and 2, respectively) [19], and No. 275451 for compound **6a**). Copies of this information may be obtained free of charge from The Director, CCDC, 12 Union Road, Cambridge CB2 1EZ, UK (Fax: +44 1223 336033; deposit@ccdc.cam.ac.uk or www.ccdc.ac.uk). Supplementary data associated with this article can be found, in the online version, at doi:10.1016/j.jorganchem.2005.07.070.

References

[1] (a) D. Bourissou, O. Guerret, F.P. Gabbaie, G. Bertrand, Chem. Rev. 100 (2000) 39;
(b) W.A. Herrmann, Angew. Chem. Int. Ed. 41 (2002) 1290.
[2] (a) M.T. Powell, D.-R. Hou, M.C. Perry, X. Cui, K. Burgess, J. Am. Chem. Soc. 123 (2001) 8878;
(b) Y. Ma, C. Song, C. Ma, Z. Sun, Q. Chai, M.B. Andrus, Angew. Chem., Int. Ed. 42 (2003) 5871;
(c) L.C. Bonnet, R.E. Douthwaite, B.M. Kariuki, Organometallics 22 (2003) 4187;
(d) A. Alexakis, C.L. Winn, F. Guillen, J. Pytkowicz, S. Roland, P. Mangeney, Adv. Synth. Catal. 345 (2003) 345;
(e) D.R. Jensen, M.S. Sigman, Org. Lett. 5 (2003) 63;
(f) L.H. Gade, V. Cesar, S. Bellemin-Laponnaz, Angew. Chem., Int. Ed. 43 (2004) 1014;
(g) E. Bappert, G. Helmchen, Synlett (2004) 1789;
(h) P.L. Arnold, M. Rodden, K.M. Davis, A.C. Scarisbrick, A.J. Blake, C. Wilson, Chem. Commun. (2004) 1612;
(i) S. Tominaga, Y. Oi, T. Kato, D.K. An, S. Okamoto, Tetrahedron Lett. 45 (2004) 5585.
[3] (a) D.S. McGuinness, K.J. Cavell, B.W. Skelton, A.H. White, Organometallics 18 (1999) 1596;
(b) D.S. McGuinness, K.J. Cavell, Organometallics 19 (2000) 741;
(c) A.M. Magill, D.S. McGuinness, K.J. Cavell, G.J.P. Britovsek, V.C. Gibson, A.J.P. White, D.J. Williams, A.H. White, B.W. Skelton, J. Organomet. Chem. 617–618 (2001) 546;
(d) T. Weskamp, W.C. Schattenmann, M. Spiegler, W.A. Herrmann, Angew. Chem. 110 (1998) 2631;
(e) T. Weskamp, F.J. Kohl, W. Hieringer, D. Gleich, W.A. Herrmann, Angew. Chem. 111 (1999) 2573;
(f) L. Ackermann, A. Fürstner, T. Weskamp, F.J. Kohl, W.A. Herrmann, Tetrahedron Lett. 40 (1999) 4787;
(g) T. Weskamp, F.J. Kohl, W.A. Herrmann, J. Organomet. Chem. 582 (1999) 362;
(h) M. Scholl, S. Ding, C.W. Lee, R.H. Grubbs, Org. Lett. 1 (1999) 953;
(i) M. Scholl, T.M. Trnka, J.P. Morgan, R.H. Grubbs, Tetrahedron Lett. 40 (1999) 2247;
(j) C.W. Bielawski, R.H. Grubbs, Angew. Chem. 112 (2000) 3025;
(k) T.M. Trnka, R.H. Grubbs, Acc. Chem. Res. 34 (2001) 18;
(l) R.H. Grubbs, Handbook of Metathesis, Wiley–VCH, Weinheim, 2003;
(m) H.M. Lee, D.C. Smith Jr., Z. He, E.D. Stevens, C.S. Yi, S.P. Nolan, Organometallics 20 (2001) 794.
[4] (a) R.W. Drumwright, P.R. Gruber, D.E. Henton, Adv. Mater. 12 (2000) 1841;
(b) M. Okada, Prog. Polym. Sci. 27 (2002) 87.
[5] (a) O. Dechy-Cabaret, B. Martin-Vaca, D. Bourissou, Chem. Rev. 104 (2004) 6147;
(b) B.J. O'Keefe, M.A. Hillmyer, W.B. Tolman, J. Chem. Soc. Dalton Trans. (2001) 2215.
[6] (a) N. Spassky, M. Wisniewski, C. Pluta, A. Le Borgne, Macromol. Chem. Phys. 197 (1996) 2627;
(b) A. Bhaw-Luximon, D. Jhurry, N. Spassky, Polym. Bull. 44 (2000) 31;
(c) D. Jhurry, A. Bhaw-Luximon, N. Spassky, Macromol. Symp. 175 (2001) 67;
(d) C.P. Radano, G.L. Baker, M.R. Smith III, J. Am. Chem. Soc. 122 (2000) 1552;
(e) T.M. Ovitt, G.W. Coates, J. Am. Chem. Soc. 124 (2002) 1316;
(f) Z. Zhong, P.J. Dijkstra, J. Feijen, J. Am. Chem. Soc. 125 (2003) 11291;
(g) N. Nomura, R. Ishii, M. Akakura, K. Aoi, J. Am. Chem. Soc. 124 (2002) 5938;
(h) K. Majerska, A. Duda, J. Am. Chem. Soc. 126 (2004) 1026;
(i) J. Belleney, M. Wisniewski, A. Le Borgne, Eur. Polym. J. 40 (2004) 523;
(j) P. Hormnirun, E.L. Marshall, V.C. Gibson, A.J.P. White, D.J. Williams, J. Am. Chem. Soc. 126 (2004) 2688.
[7] B.M. Chamberlain, M. Cheng, D.R. Moore, T.M. Ovitt, E.B. Lobkovsky, G.W. Coates, J. Am. Chem. Soc. 123 (2001) 3229.
[8] M.H. Chisholm, C.-C. Lin, J.C. Gallucci, B.-T. Ko, Dalton Trans. (2003) 406.
[9] For recent relevant examples, see (a) C.K. Williams, L.E. Breyfogle, S.K. Choi, W. Nam, V.G. Young Jr., M.A. Hillmyer, W.B. Tolman, J. Am. Chem. Soc. 125 (2003) 11350;
(b) L.M. Alcazar-Roman, B.J. O'Keefe, M.A. Hillmyer, W.B. Tolman, Dalton Trans. (2003) 3082;
(c) C.K. Williams, N.R. Brooks, M.A. Hillmyer, W.B. Tolman, Chem. Commun. (2002) 2132;
(d) B.J. O'Keefe, L.E. Breyfogle, M.A. Hillmyer, W.B. Tolman, J. Am. Chem. Soc. 124 (2002) 4384.
[10] (a) A.J. Arduengo III, H.V. Rasika Dias, F. Davidson, R.L. Harlow, J. Organomet. Chem. 462 (1993) 13;
(b) A.J. Arduengo III, F. Davidson, R. Krafczyk, W.J. Marshall, M. Tamm, Organometallics 17 (1998) 3375.
[11] D. Wang, K. Wurst, M.R. Buchmeiser, J. Organomet. Chem. 689 (2004) 2123–2130.
[12] H.S. Kim, J.J. Kim, H. Kim, H.G. Jang, J. Catal. 220 (2003) 44–46.
[13] T.R. Jensen, L.E. Breyfogle, M.A. Hillmyer, W.B. Tolman, J. Chem. Soc. Chem. Commun. 21 (2004) 2504.
[14] M.C. Law, K.-Y. Wong, T.H. Chan, Green Chem. 6 (2004) 241.
[15] See supporting information.
[16] (a) M.T. Bell, B.E. Padden, A.J. Paterick, K.A.M. Thakur, R.T. Kean, M.A. Hillmyer, E.J. Munson, Macromolecules 35 (2002) 7700;
(b) H.R. Kricheldorf, C. Boettcher, K.U. Toennes, Polymer 33 (1992) 2817.
[17] (a) E. Peris, R.H. Crabtree, Coord Chem. Rev. 248 (2004) 2239–2246;

(b) A.W. Waltman, R.H. Grubbs, Organometallics 23 (2004) 3105–3107;
(c) A.O. Larsen, W. Leu, C.N. Oberhuber, J.E. Campbell, A.H. Hoveyda, J. Am. Chem. Soc. 126 (2004) 11130–11131;
(d) P.L. Arnold, M. Rodden, C. Wilson, Chem. Commun. 13 (2005) 1743–1745.

[18] B. Cetinkaya, E. Cetinkaya, J.A. Chamizo, P.B. Hitchcock, H.A. Jasim, H. Kucukbay, M.F. Lappert, J. Chem. Soc., Perkin Trans. 1 (1998) 2047–2054.

[19] Complex **9** crystallized in two forms, and X-ray crystal structure determinations were performed for both. In form 2, significant disorder of the main molecule was observed which required fixing of key bond distances to obtain a reasonable solution; thus, we show the information for form 1 here. For further details, see the supporting information and the CIFs.

[20] (a) G.W. Nyce, T. Glauser, E.F. Connor, A. Moeck, R.M. Waymouth, J.L. Hedrick, J. Am. Chem. Soc. 125 (2003) 3046;
(b) E.F. Connor, G.W. Nyce, M. Myers, A. Moeck, J.L. Hedrick, J. Am. Chem. Soc. 124 (2002) 914.

[21] A.J. Arduengo III, R. Krafczyk, R. Schmutzler, H.A. Craig, J.R. Goerlich, W.J. Marshall, M. Unverzagt, Tetrahedron 55 (1999) 14523.

[22] D.S. McGuinness, K.J. Cavell, Organometallics 19 (2000) 741.

[23] B.E. Ketz, A.P. Cole, R.M. Waymouth, Organometallics 23 (2004) 2835–2837.